FABRICATED Fe-Mn NANOWIRE AS A BINARY OXIDE BY HYDROTHERMAL TREATMENT

Samara J. Mohammad*, Fadhil Abd Rasin**

*Department of Physic, /College of Science for women/ University of Baghdad , Samaraj_phy@yahoo.com

**Department of Physics, College of Science/ University of Baghdad, Farscien2007@yahoo.com

ABSTRACT: *Fe-Mn binary oxide with (1:1)Fe:Mn molar ratios was synthesized by a simultaneous oxidation and co-precipitation process. X-Ray Diffraction (XRD) study indicated the formation of nanostructure, strain and dislocations was studied by Williamson Hall. Hydrothermal treatment method give us nanowire structure Fe-Mn (1:1)N.W. morphology of obtained materials was showed by scanning Electron Microscopy (SEM) , imagej program using to compute average particle size average diameter size (30-60)nm for nanoparticles, average length~(1500-2000)nm and the average diameter 63nm of nanowire. Energy Dispersive X Ray Spectrometry (EDS) spectra showed strong peaks of Fe ,Mn and O for Fe-Mn binary oxide.*

Keywords: Fe-Mn nanowire, oxidation and co-precipitation, dislocations

INTRODUCTION:

Metal oxide nanowires such as TiO_2 [1], SiO_2[2], and Fe_2O_3 [3,4], have attracted much attention because of their novel applications of nanowires in Magnetic Resonance Imaging, photoluminescence, light sensing and water treatment, so materials science and nanotechnology has expanded rapidly. The inevitable intersection of these three disciplines has set in motion the development of an emerging research area, Magnetic porous Fe–Mn binary oxide nanowires were success-fully fabricated[5]. a variety of synthesis approaches have been developed to produce high quality nanoparticles Generally, nanomaterials should be stable to avoid aggregation [6]. a novel Fe−Mn binary oxide sorbent has been successfully developed, exhibiting high effectiveness in removing. The magnetite can be synthesized by various methods, including: ultrasound irradiation [7], sol-gel [8],thermal decomposition[9] and co-precipitation [10,11]. Thermal decomposition and co-precipitation are most commonly used

2. EXPERIMENTAL SECTION

2.1. Materials

Chemicals used were of analytical grade. Reaction vessels (glass) were cleaned with 1% HNO_3 and rinsed several times with deionized water before use. iron(II) Sulfate heptahydrate $FeSO_4.7H_2O$,Chaina Potassium $KMnO_4$ permanganate, panreac spain.

2.2. Preparation of Fe oxide and Fe–Mn binary oxides Fe–Mn binary oxides was synthesized at molar ratio(1:1). The Fe–Mn binary oxide with a molar ratio of 1:1was prepared according to a method slightly modified from that proposed by G.S.Zhang *et al.* [6]. A mixture of Potassium permanganate($KMnO_4$) and iron(II) sulfate) in the ratio 1:1 (0.015) plus heptahydrate ($FeSO_4.7H_{2)}$ were dissolved in 200 mL of deionized water. Under vigorous magnetic stirring, the $FeSO_4$ solution was added into the $KMnO_4$ solution simultaneously with 4 M NaOH solution to maintain he pH of the solurion in the range 7 and 8. The suspension was then stirred for 1 h, aged at room temperature for 4 h, and then washed repeatedly with deionized water until no sulfate could be detected. The suspension was then filtrated and dried at 65 ˚C for 24 h. The dry material was crushed and stored in a desiccator for futher use. The synthesis of Fe–Mn nanowire by using hydrothermal treatment method Basic Solution was prepare from 50ml of 8M NaOH with 1 g of binary oxide prepared, maintaining temprature at 170˚C by using an oven controlled temperature and time of reaction was 10h. The precipitates were formed in down of Teflon (nano wire) and then filtered, washed repeatedly with deionized water, and dried at 65˚C for 24h.

2.3 Characterization. Structure factors, Morphology, composition components

Subjected to X-Ray Diffraction (Cu Kα radiation 40 kVand 30 mA) the pattern of particles w recorded. . The microscopic morphologies of the synthesized Fe−Mn particles were observed by using a Scanning electron microscope The chemical state of elements in samples was determined by Energy Dispersive X Ray Spectrometry

Table(1) XRD data

Sample	Fe:Mn (1:1)	Fe:Mn (1:1)N.W.
2θ (Deg)	**35.518 62.7234**	**33.963 9 64.4729**
4sin θ	**1.221 2.081**	**1.168 2.133**
cos θ	**0.956 0.855**	**0.956 0.845**
Plane (hkl)	**(311) (440)**	**(311) (400)**
Interplaner Spacing d(Å)	**2.52542 1.47460**	**2.63738 1.44409**
β FWHM (Rad)	**0.0741 0.0520**	**0.0750 0.0433**

3. RESULTS AND DISCUSSION.

X-ray diffraction pattern of Fe–Mn binary oxide is illustrated in Fig. 1. The pattern with two high broad peaks at 35.4 and 62.52, identified according to d spacing of 0.253 and 0.148 nm, respectively, are eventually of magnetite[12,13].

The patterns of Fe–Mn binary oxides with Fe: Mn molar ratio 1:1 nanowire, is shown in Fig. 2

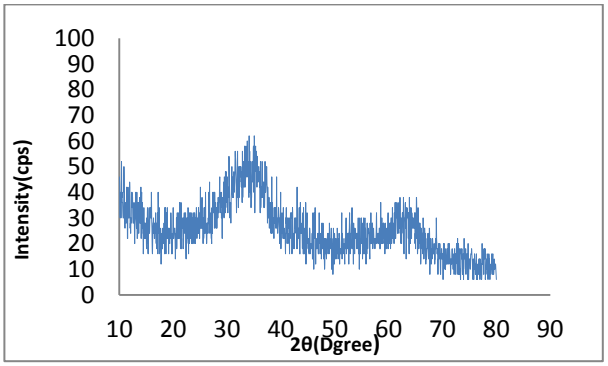

Fig (1) The X-Ray diffraction pattern of sample prepared

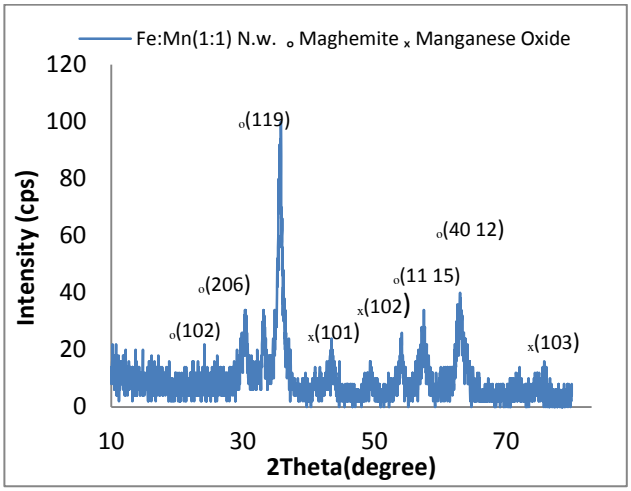

Fig. (2) X –Ray diffraction Fe-Mn (1:1)nanowire

3.1crystallite Particle Size Calculation

From this study, considering the peak at degrees, average crystallite particle size has been estimated by using Debye-Scherer formula. Inter-planar spacing between atoms (d-spacing) is calculated
using *Bragg's Law* and enumerated in Table.1.

$\boldsymbol{D = k\lambda\ /\ (\beta\ cos\ \theta\ )}$.....(1)

$\boldsymbol{d_{hkl} = n\lambda/(2\ \sin\ \theta)}$.....(2)

where, $\boldsymbol{\lambda}$ is wave length for CuK_{α} radiation (0.1540 nm), $\boldsymbol{\beta}$ is FWHM (full width at half maximum), $\boldsymbol{\theta}$ is diffraction angle, d is d-spacing , **k** is the geometric factor related to crystallite shape equal to 0.89and D is crystallite size shown in table 2.

Table(2) structure factors

Sample	Fe:Mn (1:1)	Fe:Mn (1:1)N.W.
crystallite size D (nm)	**2.29**	**2.53**
strain $\boldsymbol{\varepsilon_s}$	**0.102**	**0.1137**
Dislocation Density (m^2)	**1.9×10^{17}**	**1.56×10^{17}**

3.2. Instrumental Broadening

An appreciable broadening in diffraction pattern was observed with article size is less than 100 nm. The broadening is attributed to particle size and strain.
The observed line broadening is eventually used to estimate the average size of the particles.

The total broadening of the diffraction peak is, hwever, due to sample and the instrument. The sample broadening is described by

$\boldsymbol{\beta_{hkl}\cos\theta = \left(\frac{k\lambda}{D}\right) + (4\varepsilon_s\ \sin\theta\ )}$.....(3)

where D is the average particle size, $\boldsymbol{\varepsilon_s}$ is strain and $\boldsymbol{\beta_{hkl}}$ is instrumental broadening The total broadening equation is thus described by the instrument-corrected broadening $\boldsymbol{\beta_D}$ corresponding to the diffraction peak of nanomaterial ,estimated, using the relation:

$\boldsymbol{\beta_D^2 = [(\beta^2)_{measured} - (\beta^2)_{instrumental}]}$..(4)

The size and strain of the experimentally observed broadening of several peaks are computed simultaneously using *least squares method* and presented in Fig.3. When, particle size becomes smaller, due to size effect, the peaks become broad and widths larger. The broadening of peak may also occur due to micro strains of the crystal structure arising from defects like dislocation and twinning [14,15]. NWs possessing a cubic structure tend to coalesce into the bicrystalline or tricrystalline NWs whereas NWs with the hexagonal structure prefer to grow as single-crystalline NWs [16].
Thermal oxidation has received considerable attention because of simplicity technical and large-scale synthesis of high-quality Fe_2O_3 NWs [17, 18,19,20,21,22,23,24, 25];

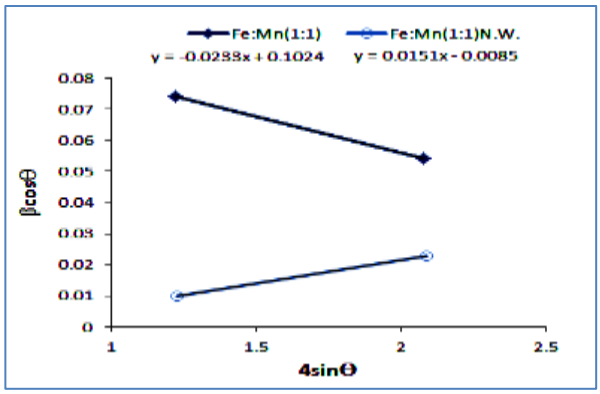

Fig.3. Williamson Hall Plot

3.3 Strain-induced broadening arising from crystal imperfections and distortion are related by $\varepsilon_s \sim \beta_s/\tan\theta$. A remarkable property of Eq. (3) is the dependency on cosθ. The W-H method does not follow a 1/cosθ dependency as in the Scherrer equation, but instead varies with tanθ. This fundamental difference allows for a separation of reflection broadening when both microstructural causes - small crystallite size and microstrain - occur together. The different approaches illustrated below assume the size and strain broadening are additive components of the total integral breadth of a Bragg peak [26]. The distinct θ dependencies of both effects are assumed to be responsible for the separation of size and strain broadening in the analysis of Williamson and Hall. Addition of the Scherrer equation and $\boldsymbol{\varepsilon_s} \sim \beta_s/\tan\theta$ results in Rearranging Eq.(3) gives the term (βcosθ) was plotted with respect to (4 sinθ) for the preferred orientation peaks of nanomaterial. Accordingly, the slope and y-intersect of the fitted line represent strain, for Fe_2O_3 NWs nucleation during the growth process, we can see shear stress could be produced inside the

Fe_2O_3 NWs. Fe_2O_3 NWs become longer, and the stress becomes larger. When the shear stress accumulates to some extent will form in the Fe_2O_3 NWs. Eventually, the modulated structures accompany with the formation the single-crystalline NWs[16].so the negative strain means uniaxial compressions and positive strain means uniaxial expansion.

3.4 the dislocation density ($\boldsymbol{\delta}$) which represents the amount of defects in the sample in table 2 is calculated using the relation [27]:

$$\boldsymbol{\delta = 1/D^2} \ldots\ldots\ldots\ldots\ldots\ldots\ldots\ldots\ldots (\mathbf{5})$$

According to Eq.(5) there is inverse relation between dislocation density and crystallite size so that dislocation density increases when the values of crystallite size decreases, when the dislocation density increases, that means there is strong strain happened with the grain. This behavior is very clear in figures1 and 2 because the peak intensity decreases and the broadening increase with decreasing Fe oxide concentration so nanocrystalline diameter decreases with an increase in crystallite size.

The strain, which is calculated from the slope of (W-H) plot; as well as the dislocation density which is calculated from Eq(5) increases with decreasing the crystallite size.

3.5 Morphology and composition components

In order to investigate the morphology of obtained materials by SEM. Fig. 4. shown SEM image of Fe–Mn binary oxides samples , in the picture appears that Nano crystalline particles composed of small particle from which we can know that the diameter size 62.5nm. The control of the monodisperse size is very important because the properties of nano crystal strongly depend upon the dimension of nanoparticles[28]. nanoparticles have spherical shape. In some places, various sizes of the particles (small and large size) are observed, A cluster of agglomerated particles can clearly be seen, so shows the average length~(1500-2000)nm and the average diameter 63nm of nanowire, the values were calculated according imagej program.

in fig(4,5,6and7). EDS spectrum showed the strong peaks of Fe,Mn and O. The composition components of particulate nanocomposite formed by co-precipitation synthesis Fe, Mn and O. These results demonstrate the purity of the synthesis results and small amount of carbon contamination which is due to the carbon tape).

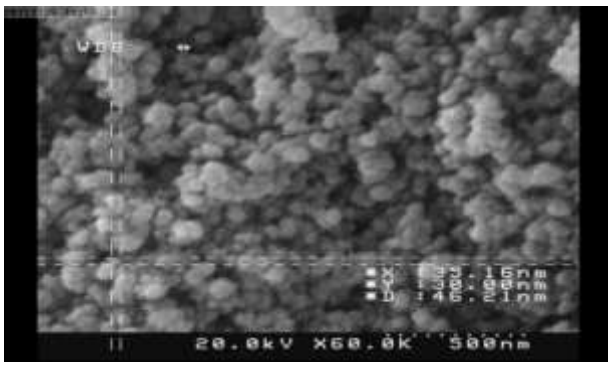

Fig (4) SEM images of of Fe-Mn (1:1)

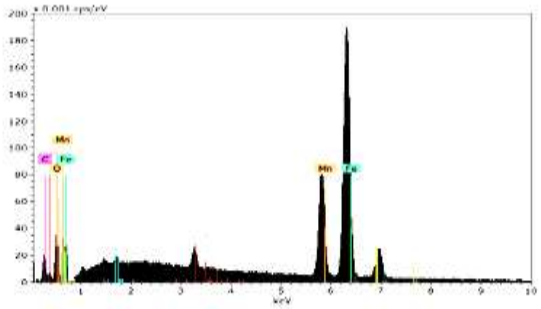

Fig(5) EDS spectrum for Fe:Mn (1:1)nanoparticles

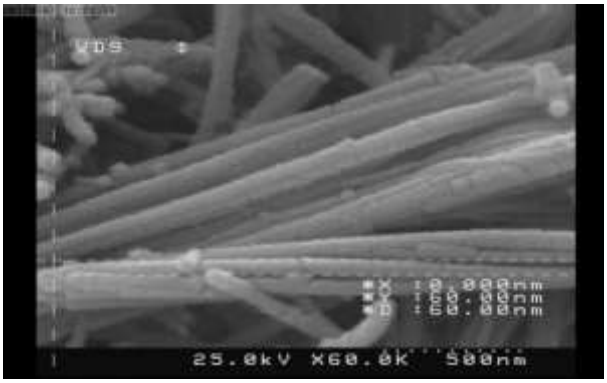

Fig (6) SEM images of of Fe-Mn (1:1) NWs

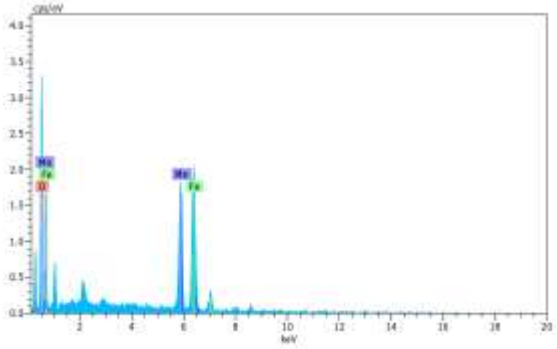

Fig(7)EDS spectrum for Fe:Mn (1:1) NWs

4. CONCLUSIONS

A cheap co-precipitation method has been used to synthesize nanoparticles of Fe–Mn binary oxides. The resulting nanoparticles determines the formation of structure factors whose average size is affected by the size of individual particles. in fact, in bigger particles so the degree of agglomeration related with strain of particle, NWs nucleation during the growth process by hydrothermal treatment of nanoparticles in 170 ˚C for 10h . SEM show nanoparticles and nano wires and EDS spectrum shown the strong peaks of Fe,Mn and O.

REFERENCE:

1.SHYUE J J, PADTURE N P. Template directed, near-ambient synthesis of Au-TiO_2-Au heterojunction nanowires mediated by self-assembled monolayers ***(SAMs)*** **[J].** Materials Letters, 2007,61(1): 182-185.

2. BUDAK S, MIA0 G X, OZDEMIR M, CHETRY K B, GUPTA A.Growth and characterization of single crystalline tin oxide (SnO_2)nanowires [J]. Journal of Crystal Growth, (2006),2: 405-41 1.

3.Srivastava H, Tiwari P, Srivastava AK, Nandedkar RV (2007) Growth and characterization of a-Fe_2O_3 nanowires. J ApplPhys 102:054303

4.Wang RM, Chen YF, Fu YY, Zhang H, Kisielowski C (2005a) Bicrystalline hematite nanowires. J Phys Chem B 109: 12245–12249

5.Hao-Jie Cuia, Jie-Kui Caia,b, Huan Zhao Fabrication of magnetic porous Fe–Mn binary oxide nanowires withsuperior capability for removal of As(III) from water"*Journal of Hazardous Materials* 279,26–31 ,(2014).

6. Zhang, G. S.; Qu, J. H.; Liu, H. J.; Liu, R. P.; Wu, R. C. Preparation and evaluation of a novel Fe−Mn binary oxide adsorbent for effective arsenite removal*". Water Res*, **41**, 1921−1928 (2007).

7. Teo, B.M.; Chen, F.; Hatton, T.A.; Grieser, F.; Ashokkumar, M. Novel one-pot synthesis of magnetite latex nanoparticles by ultrasound irradiation*". Langmuir* **25**, 2593–2595(2009).

8. Teja, A.S.; Koh, P. Synthesis, properties, and applications of magnetic iron oxide nanoparticles". *Prog. Cryst. Growth Charact. Mater* **55**, 22–45. .(2009)

9. Lu, X.; Niu, M.; Qiao, R.; Gao, M. Superdispersible PVP-coated Fe_3O_4 nanocrystals prepared by a "one-pot" reaction". J. Phys. Chem. B112, 14390–14394(2008).

10. Mizukoshi, Y.; Shuto, T.; Masahashi, N.; Tanabe, S. Preparation of superparamagneticmagnetite nanoparticles by reverse precipitation method: Contribution of sonochemicallygenerated oxidants". Ultrason. Sonochem. 16, 525–531(2009).

11. Bandhu, A.; Mukherjee, S.; Acharya, S.; Modak, S.; Brahma, S.K.; Das, D.; Chakrabarti, P.K. Dynamic magnetic behavior and Mössbauer effect measurements of magnetite nanoparticles prepared by a new technique in the co-precipitation method". *Solid State Commun*. 149, 1790–1794(2009).

12. A. Hofmann, M. Pelletier, L. Michot, A. Stradner, P. Schurtenberger, R. Kretzschmar, *J. Colloid Interface Sci.* 271 (2004) 163–173.

13. Maria Cristina Mascolo 1,2,*, Yongbing Pei 1,3 and Terry A.Room temperature co precipitation synthesis of Magnetite Nanoparticles in alarge PH Window with different bases" Ring Materials 6, 5549-5567 (2013),

14. Thamaphat K, Limsuwan P, Ngotawornchai B. Phase Characterization of TiO2 Powder by XRD and TEM. Kasetsart.J.(Nat. Sci.). 42: 357-361(2008).

15. Ghosh SC, Thanachayanont C, Dutta J. Studies on Zinc sulphide nanoparticles for Field Emission Devices. The 1st ECTI Annual Conference ECTI-CON Pattaya, Thailand;p.145-148. (2004) .

16. R. S. Cai • T. Li • Y. Q. Wang Formation of modulated structures in single-crystallinehexagonal a-Fe_2O_3 nanowiresJ Nanopart Res (2012) 14:1073

17.Chen ZQ, Cvelbar U, Mozetic M, He JQ, Sunkara MK (2008b)Long-range ordering of oxygen-vacancy planes in a-Fe_2O_3 nanowires and nanobelts. Chem Mater 20:3224–3228

18.Chueh YL, Lai MW, Liang JQ, Chou LJ, Wang ZL (2006) Systematic study of the growth of aligned arrays of α-Fe_2O_3 and Fe_3O_4 nanowires by a vapor–solid process. Adv

19.Cvelbar U, Chen ZQ, Sunkara MK, Mozetic M (2008) Spontaneous growth of superstructure a-Fe2O3 nanowire and nanobelt arrays in reactive oxygen plasma. Small 4: 1610–1614

20.Dong Z, Kashkarov P, Zhang H (2010) Monte Carlo study forthe growth of a-Fe2O3 nanowires synthesized by thermal oxidation of iron. Nanoscale 2:524–528

21.Han Q, Liu ZH, Xu YY, Chen ZY, Wang TM, Zhang H (2007)Growth and properties of single-crystalline Fe_2O_3 nanowires. J Phys Chem C 111:5034–5038

22.Hiralal P, Unalan HE, Wijiayantha KGU, Kursumovie A, Jefferson D, MacManus-Driscoll JL, Amaratunga GAJ (2008) Growth and process conditions of aligned and patternable films of iron(III) oxide nanowires by thermal oxidation of iron. Nanotechnology 19:455608

23.Nasibulin AG, Rackauskas S, Jiang H, Tian Y, Mudimela PR, Shandakov SD, Nasibulina LI, Sainio J, Kauppinen EI (2009) Simple and rapid synthesis of a-Fe2O3 nanowires under ambient conditions. Nano Res 2:373–379

24.Rachauskas S, Nasibulin AG, Jiang H, Tian Y, Kleshch VI, Sainio J, Obraztsova ED, Bokova SN, Obraztsov AN, Kauppinen EI (2009) A novel method for metal oxide nanowire synthesis. Nanotechnology 20:165603

25.Wen XG, Wang SH, Ding Y, Wang ZL, Yang SH (2005) Controlled growth of large-area, uniform, vertically aligned arrays of a-Fe_2O_3 nanobelts and nanowires. JPhys Chem B, 109:215

26.Sirdeshmukh DB, Sirdeshmukh L, Subhadra KG. Micro- and Macro-Properties of solids:Thermal, Mechanical and Dielectric properties. *Springer, NewYork.*(2006).

27. Chinh NQ, Gubicza J, Langdon TG. Characteristics of face-centered cubic metals processed by equal-channel angular pressing". *J.Mater.Sci.* **42**(5): 1594-1605(2007).

28. Poedji Loekitowati Hariani, Muhammad Faizal, Ridwan, Marsi, and Dedi Setiabudidaya *nternational Journal of Environmental Science and Development*, (**4)** 3 (2013)